Solvent-Dependent Photophysics of 1-Cyclohexyluracil: Ultrafast Branching in the Initial Bright State Leads Nonradiatively to the Electronic Ground State and a Long-Lived $^1n\pi^*$ State

Patrick M. Hare, Carlos E. Crespo-Hernández, and Bern Kohler*

Department of Chemistry, The Ohio State University, 100 West 18th Avenue, Columbus, Ohio 43210

Received: July 24, 2006

The modified nucleic acid base, 1-cyclohexyluracil, was studied by femtosecond transient absorption spectroscopy in protic and aprotic solvents of varying polarity. UV excitation at 267 nm populates the lowest-energy bright state, a $^1\pi\pi^*$ state, which has a lifetime of 120−270 fs, depending on the solvent. In all solvents, this initial bright state population bifurcates with ∼60% undergoing subpicosecond nonradiative decay to the electronic ground state and the remaining population branching to a singlet dark state. The latter absorbs between 340 and 450 nm. The latter state is assigned to the lowest-energy $^1n\pi^*$ state. It decays to the electronic ground state with a lifetime that varies from 26 ps in water to at least several nanoseconds in aprotic solvents. The results suggest that the two nonradiative decay pathways identified for photoexcited uracil in recent quantum chemical calculations (Matsika, S. *J. Phys. Chem. A.* **2004**, *108*, 7584) are simultaneously operative in a wide variety of solvent environments. The lowest-energy triplet state was also detected by transient absorption. The triplet population appears in a few picoseconds and is not formed from the thermalized $^1n\pi^*$ state. It is suggested that high spin−orbit coupling is found only along initial segments of the nonradiative decay pathways. Efficient intersystem crossing prior to vibrational cooling offers a possible explanation for the wavelength-dependent triplet yields seen in single DNA bases.

Introduction

Much that is complex about the electronic structure of single DNA and RNA bases is due to the existence of energetically proximate $^1\pi\pi^*$ and $^1n\pi^*$ excited electronic states.[1,2] Transitions to the latter states are nearly electric-dipole-forbidden, making them difficult to study using conventional spectroscopic techniques. Although they have been observed experimentally only rarely, many important roles have been ascribed to $^1n\pi^*$ states. They may be responsible for ultrafast nonradiative decay in nucleobases.[3−7] In addition, these states may mediate triplet state formation. The lowest excited electronic states of singlet and triplet multiplicity have $\pi\pi^*$ character for perhaps all of the DNA bases in aqueous solution. However, classical propensity rules indicate that interconversion between these states is hindered by low spin−orbit coupling. However, intersystem crossing (ISC) from a $^1n\pi^*$ to a $^3\pi\pi^*$ state or from a $^1\pi\pi^*$ to a $^3n\pi^*$ state is much more favorable.[8] Still, there are no experiments to our knowledge that conclusively establish the intermediacy of $^1n\pi^*$ states in ISC. Understanding how triplet states are formed is important because of the role that these long-lived states may play as precursors to various DNA photoproducts, including cyclobutane pyrimidine dimers.[9] Presently, it is impossible to account for how singlet excited states evolve to triplets, and this has impeded progress at understanding DNA photochemistry.

Here we report a comprehensive femtosecond pump−probe investigation of the excited-state dynamics of 1-cyclohexyluracil (1CHU, Chart 1). This uracil derivative was chosen because it is soluble in solvents with widely varying polarity. Generally, $^1n\pi^*$ and $^1\pi\pi^*$ states of organic chromophores respond differently to solvation, allowing the relative energies of these states to be tuned. Because triplet yields in uracil and thymine increase dramatically in less polar solvents,[10,11] this compound is an excellent choice for a study of triplet formation. We show that ultrafast internal conversion to the electronic ground state (S_0) occurs alongside ultrafast branching to what is most likely a $^1n\pi^*$ state. This latter dark state has not been detected previously in the condensed phase. Surprisingly, the dark state yield is ∼40% in all solvents. We propose a model that qualitatively explains two poorly understood aspects of nucleobase triplet states: the pronounced effect of excitation wavelength and solvent on triplet yields.

CHART 1

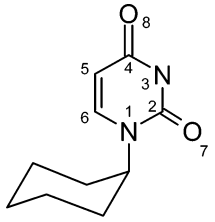

Experimental Methods

Experiments were carried out using femtosecond pump−probe spectrometers, as described previously.[12,13] Briefly, pump pulses with a center wavelength of 267 nm were obtained from the third harmonic of the output of a regeneratively amplified Ti:sapphire laser (Clark-MXR, Inc., Dexter, MI, or Coherent

* Author to whom correspondence should be addressed. E-mail: kohler@chemistry.ohio-state.edu.

10.1021/jp064714t CCC: $33.50
Published on Web 09/01/2006

Inc., Santa Clara, CA). Visible probe pulses were derived from a white light continuum generated in a 1 cm path length water cell. Wavelength selection in the visible and near UV was carried out by placing a 10 nm interference filter in the continuum beam before the sample. UV and near UV probe pulses were obtained from the output of a Coherent, Inc., optical parametric amplifier (OPA). UV probe pulses were spectrally isolated after the sample using a HORIBA Jobin-Yvon (Edison, NJ) H10-D-UV monochromator with 1 mm slits. Probe pulses were detected with either a photomultiplier tube or an amplified Si photodiode. Detector signals were sent to a Stanford Research Systems (Sunnyvale, CA) SRS830-DSP lock-in amplifier referenced to an optical chopper in the pump pulse path. Most measurements were made in this way at single probe wavelengths, but broadband transient absorption spectra were also recorded with 282 nm excitation and probing between 340 and 700 nm by means of a supercontinuum pulse and an imaging spectrometer equipped with a charge coupled device (CCD) detector.

Pump pulse intensities were typically between 0.2 and 2 GW cm^{-2} at the sample. The probe pulse diameter at the sample was 3−5 times smaller than that of the pump. Transients were recorded in aerated solutions unless otherwise indicated. Solutions were spun at several hundred revolutions per minute (RPMs) in a 1.2 mm path length spinning cell with calcium fluoride windows. Solutions were prepared to have an absorbance of ∼1 in the sample cell at the pump wavelength, corresponding to solute concentrations of ∼0.5−1 mM. Samples were monitored for photodegradation by UV−vis absorption spectroscopy during the measurements. Spectrophotometric grade acetonitrile, *n*-butanol, methanol, and carbonyl-free ethyl acetate were obtained from VWR International (West Chester, PA) and used as received. 1CHU, D_2O (99.9 at. %), and 3-methyladenine were obtained from Sigma-Aldrich (St. Louis, M)) and used as received. 2,2,2-Trifluoroethanol (99.8%) was obtained from Acros Organics USA (Morris Plains, NJ) and doubly distilled prior to use.

In control experiments, several of the neat solvents exhibited transient absorption signals. Most solvents gave a coherent spike centered about $t = 0$. This feature increases in intensity with decreasing probe wavelength and is caused by simultaneous absorption of one pump and one probe photon by the solvent.[14] The second feature is transient absorption at positive delay times due to solvated electrons produced from two-photon ionization of the solvent. The amplitude of this feature decreases with decreasing probe wavelength and is negligible at $\lambda \leq 400$ nm. This signal contribution arises solely from the solvent and was removed using a subtraction procedure similar to that used in previous experiments.[15] Briefly, transients were recorded on equal absorbance solutions of 1CHU and 3-methyladenine in the solvent of interest. Since the lifetime of 3-methyladenine is subpicosecond in every solvent used in this study at $\lambda > 400$ nm (ref 12 and unpublished data), any detectable offset at times greater than a few picoseconds arises from multiphoton ionization of the solvent. The solvent-only transient absorption signal was scaled to match the long-time signal of the 3-methyladenine trace and then subtracted from the 1CHU signal. This procedure isolated true solute dynamics from signals due to the solvent.

All transient decays were globally fitted to a sum of exponentials convoluted with a Gaussian instrument response function using a routine included in IGOR Pro 5.04 (Wavemetrics, Inc., Lake Oswego, OR). The full width at half-maximum (fwhm) of the instrument response function was fixed at 250 and 200 fs for the Clark-MXR, Inc., and Coherent Inc. spectrometers, respectively, based on fitting to the solvent-only scans. In general, three exponentials were sufficient to fit transients at any probe wavelength. Reported uncertainties are consistently twice the standard error. No attempt was made to correct for the coherent spike centered about $t = 0$ (seen mostly at UV and near UV probe wavelengths), and this region was excluded from the fitted region.

Experiments on deaerated solutions were carried out by flowing ∼50 mL of the solution under study through a 0.5 mm or 1 mm path length fused silica cell using a laboratory pump. Dry Ar or N_2 gas was bubbled through the solution during measurements. The large solution volume minimized the change in concentration due to solvent evaporation. However, aliquots of neat solvent were added periodically to maintain the starting volume during long data runs.

TABLE 1: Steady-State Absorption Data for 1CHU in a Variety of Solvents

		λ_{max} (nm)		
solvent	ϵ_r[a]	1CHU	Ura	α[b]
pH 6.8 buffer	80.1	269	259	1.17
acetonitrile	36.6	266	256	0.19
methanol	33.0	267	259	0.93
2,2,2-trifluoroethanol	27.7	268		1.51
n-butanol	17.8	267	259	0.79
ethyl acetate	6.1	265		0

[a] ϵ_r = dielectic constant from ref 70. [b] α = Kamlet−Taft parameter from ref 18.

Results

Steady-State Absorption Spectra. In pH 7 buffer solution, the steady-state absorption spectrum of 1CHU is red-shifted 10 nm from that of uracil (Table 1). An 8 nm red shift is seen for 1-methyluracil.[16] As the hydrogen-bond-donating acidity of the solvent decreases (as measured by the Kamlet−Taft α parameter[17,18]), the absorption maximum of 1CHU shifts to shorter wavelengths ($\Delta_{max} = 4$ nm between pH 7 buffer and ethyl acetate). A comparable blue shift was observed for uracil in buffer solution, ethanol, and ethyl ether.[19]

Transient Absorption in Aprotic Solvents. Acetonitrile and ethyl acetate were chosen as aprotic solvents with intermediate and low dielectric constants (Table 1), respectively. Transients recorded over a broad range of probe wavelengths reveal complex multiexponential decays. Signals for 1CHU in acetonitrile are shown in Figure 1. Global fit parameters for both solvents are given in Table 2. The shortest time constant (τ_1) has approximately the same value in both solvents within experimental uncertainty. For this component, positive amplitudes indicating decays are observed at probe wavelengths ≥500 nm, while negative amplitudes indicating rising signals are seen at 400−450 nm in acetonitrile. At these wavelengths in ethyl acetate, the rise was obscured by the coherent time zero signal from the solvent. Although only relative amplitudes are given in Tables 2 and 3, back-to-back experiments performed with constant laser parameters showed that the τ_1 decay has the largest absolute amplitude near 600 nm.

Several nanoseconds after the pump pulse, a residual signal is present at all probe wavelengths. In ethyl acetate, the transients at wavelengths greater than 500 nm decay with a time constant of 4 ± 2 ns. Below 500 nm, the signal shows negligible decay at 3.5 ns and was fit to a constant offset ($\tau_3 = \infty$). In acetonitrile, the long-time signal decayed with a time constant of 3.2 ± 0.2 ns at all probe wavelengths. When oxygen was removed from the solution by deaeration, the long-time signal showed almost

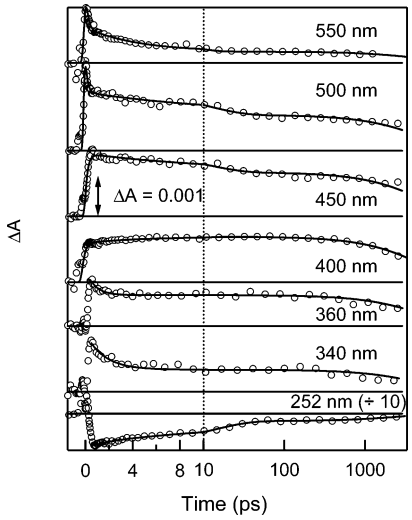

Figure 1. Transient absorption traces of 1CHU in acetonitrile probed at wavelengths from 252 to 550 nm. Solid curves are from global fits to the data. Fit parameters are listed in Table 2.

TABLE 2: Best-Fit Time Constants and Relative Amplitudes (in Parentheses) for 1CHU Transient Absorption Signals in Aprotic Solvents[a]

solvent	λ (nm)	τ_1 (ps)	τ_2 (ps)	τ_3 (ns)
acetonitrile	252[b]		9.1 ± 0.4 (−76)	3.2 ± 0.2 (−24)
	280[b]		" (−63)	" (−37)
	340[b]		1.4 ± 1 (62)	" (38)
	360[b]		0.7 ± 0.9 (46)	" (54)
	400	0.20 ± 0.05 (−37)	7 ± 5 (−11)	" (52)
	450	" (−49)	9 ± 8 (14)	" (37)
	500	" (50)	10 ± 8 (18)	" (32)
	550	" (56)	15 ± 5 (24)	" (20)
	570	" (63)	4 ± 2 (25)	" (12)
	610	" (69)	4 ± 2 (22)	" (9.7)
	650	" (72)	4 ± 3 (21)	" (6.4)
ethyl acetate	252[b]		11 ± 1 (−53)	∞ (−47)
	340[b]		3 ± 1 (40)	" (60)
	400[b]		4 ± 2 (−29)	" (71)
	500	0.27 ± 0.06 (86)	4 ± 2 (5.7)	4 ± 2 (8.1)
	550	" (57)	4 ± 2 (33)	" (10)
	600	" (67)	5 ± 2 (28)	" (4.7)

[a] Parameters indicated by " were linked to the parameter one row higher during global fitting. [b] Coherent spike near time zero excluded from fit.

no decay within our time window as shown in Figure 2. The amplitude of the τ_3 component decreases strongly on going from 340 to 700 nm in both solvents.

A third time constant (τ_2) intermediate between the subpicosecond (τ_1) and the long-time decay (τ_3) appears in all transients as seen in Table 2. At 252 nm, negative signals are observed corresponding to bleaching of the ground-state population. Approximately 70% of the total bleach signal in acetonitrile recovers with a time constant (τ_2) of 9.1 ± 0.4 ps. In ethyl acetate, the long-time signal has a larger amplitude relative to the initial bleach, and recovery of about half of the signal occurs with τ_2 equal to 11 ± 1 ps. At longer probe wavelengths, decays are observed with time constants between 4 and 15 ps. At wavelengths longer than about 550 nm, both solvents show decays of ∼4 ps. The relative contribution of this decay is just above 20% in acetonitrile and about 30% in ethyl acetate. This decay may be slightly longer in acetonitrile between 400 and 500 nm, but the uncertainty is great here because this is an intermediate decay of low amplitude. A transient spectrum of 1CHU in acetonitrile was recorded 50 ps after excitation (black trace, Figure 6).

Transient Absorption in Protic Solvents. Transients for 1CHU in water are shown in Figure 3. The decay at 550 nm shows only a subpicosecond decay as reported previously for uracil.[20] At shorter probe wavelengths, however, the dynamics are quite complex, as seen in the aprotic solvents. Figure 4 compares transient signals recorded at 340 nm in each protic solvent with the signal at 500 nm and with the inverted bleach signal at 252 nm. The latter two signals have been scaled to match the long-time signal at 340 nm. Comparing the signals in this way allows conclusions to be reached about kinetic decays that are independent of any fitting procedure. Decay times and amplitudes for 1CHU in pH 7 aqueous solution, 2,2,2-trifluoroethanol (TFE), methanol, and *n*-butanol are given in Table 3. Transients measured in each solvent were again globally fit to a sum of three exponentials. Fit parameters are listed in Table 3. The three time constants are tabulated in four columns such that each one has the same subscript as the one in Table 2 having the same underlying assignment. These assignments will be presented in the Discussion section.

A subpicosecond time constant of approximately 150 fs (within experimental uncertainty) is seen in all protic solvents except in aqueous solution, where this ultrafast lifetime may be somewhat shorter. As in the aprotic solvents, the subpicosecond decay has the largest relative amplitude at visible probe wavelengths. With the exception of TFE, the protic solvents undergo a small amount of photoionization due to two-photon absorption of the pump pulse. This produces solvated electrons, which have maximum absorption in these solvents between approximately 600 and 700 nm. As described in the Experimental Section, the solvated electron signal was subtracted from transients with probe wavelengths longer than 450 nm before fitting. After this subtraction procedure, nonzero signal was still observed several nanoseconds after the pump pulse. The fact that a long-lived (negative-valued) offset is observed at bleach wavelengths <300 nm, where the solvated electron does not absorb, provides evidence that the subtraction procedure does not lead to a spurious offset at longer probe wavelengths. In all solvents, the long-lived signal has the largest relative amplitude near 400 nm.

In power-dependent measurements carried out at different probe wavelengths (data not shown), the signal (solvent-subtracted signal at wavelengths where two-photon ionization is present) increased strictly linearly with the pump intensity. In TFE, methanol, and *n*-butanol, the signal shows a significant decay in the first 3 ns, while a decay is more difficult to detect in water. In the latter solvent, the longest time constant was therefore held at infinity. In those solvents where long-time signal decays were observed (TFE, methanol, and *n*-butanol), the signal became essentially constant upon deaeration.

Bleach signals in the protic solvents at 252 nm decay with three exponentials, instead of the two exponentials seen in the two aprotic solvents. The new time constant is labeled τ_4 in Table 3 and is distinctly longer than τ_2. It varies between 26 ps in water and 330 ps in *n*-butanol. In all solvents, this decay component has a relative amplitude of 30−40% at 252 nm. Positive amplitudes are observed between 300 and 400 nm in all solvents, but this component is missing in transients at probe wavelengths >450 nm.

As in the aprotic solvents, a decay component with a time constant longer than the τ_1 decay but shorter than ∼20 ps is present at virtually all probe wavelengths. At probe wavelengths where bleach signals are observed, τ_2 varies from 2 ps in water to 4.6 ps in *n*-butanol and has a relative amplitude of 50−70%. At probe wavelengths greater than 300 nm, positive τ_2 ampli-

TABLE 3: Best-Fit Time Constants and Relative Amplitudes (in Parentheses) for 1CHU Transient Absorption Signals in Protic Solvents[a]

solvent	λ (nm)	τ_1 (ps)	τ_2 (ps)	τ_3 (ns)	τ_4 (ps)
water, pH 7	252[b]		2.4 ± 0.3 (−67)	∞ (−1.2)	26 ± 2 (−32)
	280[b]		" (−52)	*c*	" (−48)
	340[b]		0.9 ± 0.3 (75)	∞ (0.90)	" (24)
	360[b]		0.3 ± 0.2 (78)	∞ (0.93)	" (21)
	400[b]			∞ (10)	" (90)
	450[d]			∞ (27)	" (72)
	500[d]	0.12 ± 0.04 (84)	13 ± 6 (9.0)	∞ (7.2)	
	550[d]	" (100)			
TFE	255[b]		4.3 ± 0.8 (−54)	3.1 ± 0.8 (−6.0)	80 ± 10 (−40)
	340[b]		0.7 ± 0.3 (79)	" (1.0)	" (20)
	380[b]		0.2 ± 0.3 (72)	" (8.4)	" (20)
	400	0.15 ± 0.02 (−29)		" (5.2)	" (66)
	450	" (−63)		" (18)	40 ± 20 (19)
	500	" (77)	20 ± 10 (8.5)	" (14)	
	550	" (87)	13 ± 9 (5.3)	" (7.5)	
methanol	252[b]		3.7 ± 0.4 (−52)	3 ± 1 (−11)	110 ± 20 (−38)
	340[b]		0.9 ± 0.2 (66)	" (9.0)	" (25)
	400[b]			" (40)	" (60)
	450[d]	0.14 ± 0.03 (48)		" (1.6)	30 ± 20 (51)
	500[d]	" (87)	4 ± 2 (8.5)	" (4.4)	
	550[d]	" (81)	2.0 ± 0.6 (14)	" (4.8)	
n-butanol	252[b]		4.6 ± 0.4 (−55)	5 ± 1 (−11)	330 ± 30 (−34)
	340[b]		0.8 ± 0.2 (68)	" (5.3)	" (27)
	380[b]		0.2 ± 0.1 (84)	" (7.6)	" (8.4)
	400[b]			" (66)	" (34)
	450[d]	0.15 ± 0.01 (88)		" (6.6)	80 ± 40 (4.8)
	500[d]	" (72)	3 ± 2 (23)	" (5.5)	
	550[d]	" (82)	4 ± 2 (5.4)	" (13)	

[a] Parameters indicated by " were linked to the parameter one row higher during global fitting. [b] Coherent spike near time zero excluded from fit. [c] Not fit due to very low amplitude. [d] Transient corrected for solvent ionization.

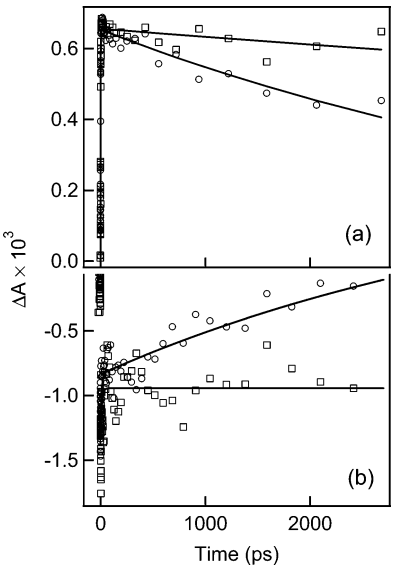

Figure 2. Back-to-back transient absorption traces of 1CHU in aerated (circles) and deaerated (squares) acetonitrile solutions at (a) 400 and (b) 250 nm. Solid lines are from fits to the transients.

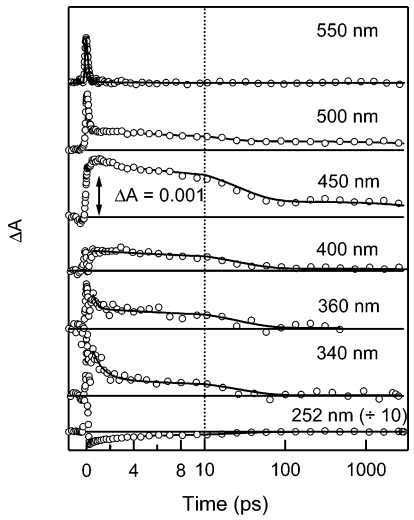

Figure 3. Transient absorption traces of 1CHU in buffered aqueous solution probed at wavelengths from 252 to 550 nm. Solid curves are from global fits to the data. Fit parameters are listed in Table 3. Transients at 450−550 nm were corrected for solvent ionization.

tudes are observed, which generally make a diminishing relative contribution to the transients as the probe wavelength is increased.

Transients in back-to-back experiments on 1CHU in H_2O and D_2O at 340 nm are shown in Figure 5. The decays match after the conclusion of the τ_2 decay, which is 1.3 times longer in D_2O than that in H_2O.

Discussion

Ultrafast Nonradiative Decay from the $^1\pi\pi^*$ State to S_0. In 2000, the $^1\pi\pi^*$ excited states of single DNA and RNA nucleosides were shown by femtosecond transient absorption measurements to have lifetimes below 1 ps.[2,21,22] Fluorescence upconversion experiments confirmed these results and established that emission from the $^1\pi\pi^*$ state is a subpicosecond process.[23−25] Recent fluorescence upconversion experiments showed that a variety of uracil derivatives have fluorescence lifetimes of ∼100 fs.[16] The shortest decay time observed in aqueous solution agrees well with this value. The decay constant τ_1, which varies between 120 and 270 fs (Tables 2 and 3), is therefore assigned to the decay of the optically populated $^1\pi\pi^*$ state of 1CHU. We note that the spectral amplitude of this

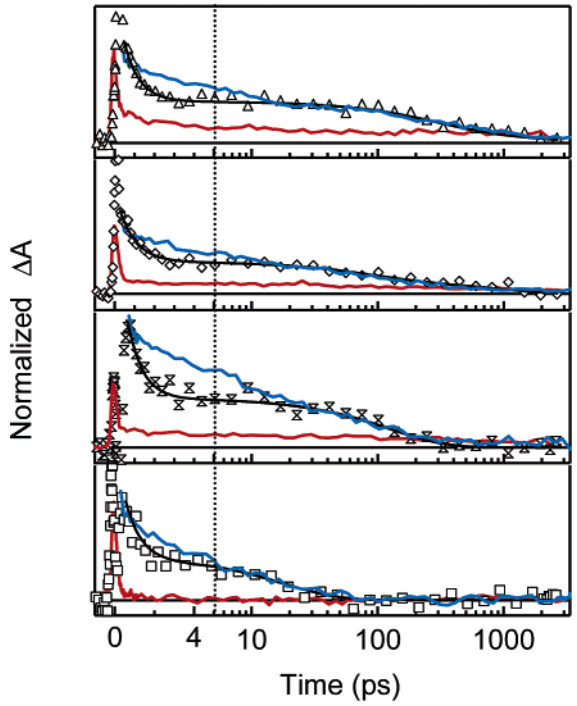

Figure 4. Transient absorption decays of 1CHU in *n*-butanol (triangles), methanol (diamonds), TFE (hourglasses), and pH 7 buffer (squares) pumped at 267 nm and probed at 340 nm. The time axis is linear for $t \leq 5$ ps and logarithmic thereafter. Solid lines are from global fits, summarized in Tables 2 and 3. The solid blue curves are signals at 252 nm in each solvent, inverted and scaled to agree with the 340 nm signal at long times. The solid red curves show signals at 550 nm in each solvent, scaled to the 340 nm signal at long times. Each of the 550 nm transients was corrected for solvent ionization, except for the TFE transient where no ionization was observed.

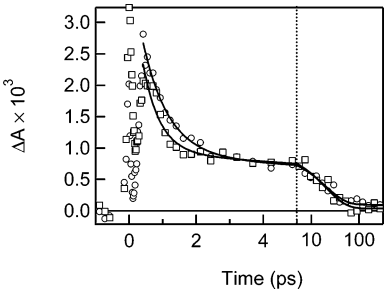

Figure 5. Transient absorption decays of 1CHU in H_2O (squares) and D_2O (circles) recorded in back-to-back experiments at a probe wavelength of 340 nm. Solid lines are best-fit curves.

component has a maximum near 600 nm in all solvents. The $^1\pi\pi^*$ states of the DNA nucleosides show maximum absorption near the same wavelength in aqueous solution,[22] supporting our assignment. In previous femtosecond transient absorption measurements, a lifetime of 0.21 ± 0.03 ps was reported for uracil and uridine. Comparison with the value here and the femtosecond fluorescence upconversion data[16] suggests that the previous measurements may have had inadequate time resolution. The results in Tables 2 and 3 show a 2-fold increase in the $^1\pi\pi^*$ lifetime upon going from protic to aprotic solvents. This increase resembles the 1.5-fold longer lifetime observed for 9-methyladenine in acetonitrile compared to that in water.[12]

Vibrational Cooling in S_0. Vibrational cooling (VC) is the process by which a solute molecule with excess vibrational energy returns to thermal equilibrium with the surrounding solvent molecules. In transient electronic spectroscopy, a vibrationally hot molecule absorbs at longer wavelengths, and

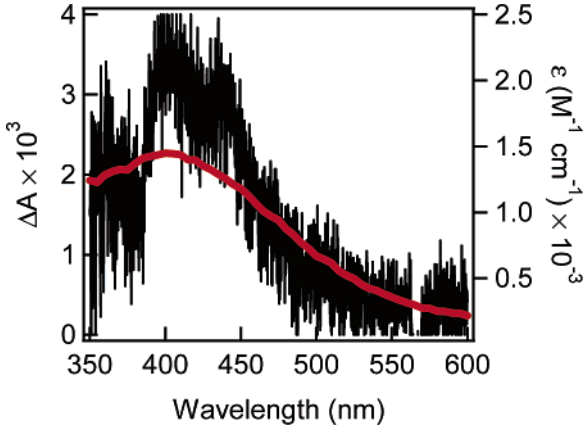

Figure 6. Transient absorption spectrum acquired at a delay of 50 ps of 1CHU in acetonitrile pumped at 282 nm (black trace, left axis) and the corrected triplet−triplet absorption spectrum of UMP in water (red trace, right axis) from ref 41.

VC reflects a progressive thermalization of energy in which the transient spectrum rapidly shifts to the blue. Generally, this results in decaying signals on the red edge and rising signals on the blue edge of the absorption spectrum. The rate of cooling is thought to depend primarily on solvent properties and varies from a few picoseconds to a few tens of picoseconds. Higher rates of cooling are observed in hydrogen-bonding solvents,[22,26] while lower rates are observed in unassociated organic liquids.[27] VC is potentially observable in any electronic state provided that the rate of formation of the nonthermal population distribution in that state (k_{pop}) is faster than the rate of cooling (k_{VC}), which in turn must be faster than the total rate of depopulation (k_{depop}), i.e., $k_{pop} > k_{VC} > k_{depop}$. This is often the case when the S_1 state of a molecule is populated by a femtosecond laser pulse, but VC dynamics are observable in other electronic states when the preceding inequality is obeyed. For example, S_0 is repopulated by ultrafast internal conversion in monomeric nucleobase molecules faster than the rate of cooling, allowing VC dynamics to be seen readily both at wavelengths slightly beyond the red edge of the S_0 absorption spectrum[21,22] and at wavelengths in the middle of the S_0 band,[13] where negative signals are observed.

Negative induced absorbance changes arise from bleaching of the ground-state population and result in the negative amplitudes at UV probe wavelengths (Tables 2 and 3). The slower decay components (τ_3 and τ_4) in the bleach recovery signal arise from additional nonradiative decay pathways that will be discussed later. Much of the bleach signal recovers with a time constant (τ_2) of several picoseconds. This is the expected signature of vibrational cooling in S_0, as seen recently in the 5′-mononucleotides of adenine and thymine.[13] For the 5′-mononucleotide of adenine, 98% of the bleach signal at 250 nm recovered with a time constant of 2.0 ps in aqueous solution.[13] In the same solvent, the bleach recovery signal at 253 nm for the 5′-mononucleotide of thymine (TMP) was characterized by a 2.4 ps time constant.[13] These values agree very well with the 2.4 ps value seen here for 1CHU in aqueous solution. The good agreement between 1CHU and TMP is notable in view of their very different $^1\pi\pi^*$ lifetimes (120 fs for 1CHU, Table 3, and 740 fs for TMP[13]). This indicates that the time scale for VC is determined predominantly by solvent properties and not by the solute's rate of nonradiative decay as long as the latter time scale is not rate-limiting.

We suggested previously that the unusually high rate of VC seen in nucleobases in aqueous solution is the result of hydrogen

TABLE 4: Intersystem Crossing (Φ_T) and Internal Conversion Yields ($\Phi_{IC,0}$) for 1-Cyclohexyluracil (1CHU), Uracil (Ura), and Uridine (Urd) in Various Solvents at the Indicated Excitation Wavelength (λ_{exc})

molecule	solvent	λ_{exc} (nm)	Φ_T	$\Phi_{IC,0}$	ref
1CHU	water	267	0.03 ± 0.02	0.62 ± 0.05	this work
1CHU	TFE	267	0.04 ± 0.05	0.55 ± 0.02	this work
1CHU	methanol	267	0.09 ± 0.06	0.55 ± 0.06	this work
1CHU	*n*-butanol	267	0.13 ± 0.05	0.56 ± 0.08	this work
1CHU	acetonitrile	267	0.34 ± 0.06[a]	0.66 ± 0.06	this work
1CHU	ethyl acetate	267	0.54 ± 0.06[a]	0.46 ± 0.06	this work
Ura	water	265	0.024		11
Ura	water	265	0.02		71
Urd	water	265	0.015		11
Ura	methanol	265	0.06		11
Ura	ethanol	265	0.1		11
Ura	acetonitrile	254	0.4		52
Ura	acetonitrile	265	0.2		10
Urd	acetonitrile	265	0.078		11
Urd	acetonitrile	254	0.3		52

[a] Upper limit, see discussion for details.

bonding to solvent molecules.[22] The trends in τ_2 in Tables 2 and 3 provide strong evidence that this is so. The rate of vibrational cooling (*n*-butanol < TFE < methanol < H_2O) increases with increasing number density of hydroxyl groups in these liquids, as discussed by Terazima.[26] This suggests that not only solute−solvent hydrogen bonds but also hydrogen bonds between solvent molecules are important for the rapid dispersal of excess vibrational energy. Interestingly, τ_2 is 1.3 times longer in D_2O compared to that in H_2O. In the two aprotic solvents, τ_2 has a distinctly longer value of ~10 ps.

Long-Lived Dark States. Ultrafast internal conversion and the subsequent vibrational cooling are well documented photoprocesses for excited nucleobase monomers in the condensed phase.[2] What is highly novel about the 1CHU transient absorption signals presented here are the additional slow decay components seen in Figures 1−4. The slow dynamics, characterized by τ_3 and τ_4 in Tables 2 and 3, cannot arise from two-photon solvent ionization because offsets are observed in solvents such as TFE and acetonitrile, which show negligible ionization at our pump wavelength due to their high gas-phase ionization potentials (~12 eV[28,29]). A further explanation for complex dynamics, which we considered but rejected, is the coexistence of two or more tautomeric forms, each having its own lifetime, as seen for adenine in aqueous solution.[12] Frequently, the lowest-energy tautomer in aqueous solution is not the minimum energy tautomer in the gas phase.[2] In the case of uracil, however, most experiments[30−35] and calculations[30,36−38] find that the diketo form is dominant in aqueous solution, in the gas phase, and in low-temperature matrixes. Reports of other tautomers[39] have later been attributed to impurities[38] or to unwarranted assumptions, such as the impossibility of fast triplet formation.[40] We assume in the following that only a single tautomer is present and ascribe all dynamics to the diketo form of 1CHU.

The complex signals seen in Figures 1−4 are due to absorption by electronic states other than the $^1\pi\pi^*$ and S_0 states. Uracil derivatives exhibit only subpicosecond emission decays,[16] so any long-lived excited states are dark, meaning that they have very low probability of radiative decay to S_0 and therefore make a negligible contribution to emission signals. One of the dark states contributing to the 1CHU signals is clearly a triplet state since removal of oxygen by deaeration causes the slowest decay time (τ_3) to become a nearly constant offset (Figure 2). Although nucleobase triplet yields are generally less than 0.01−0.02 in aqueous solution,[9] values as large as 0.2−0.4 (Table 4) are observed for uracil and its derivatives in less polar solvents.[10,11] Further evidence for triplet population comes from the good agreement between the transient spectrum (Figure 6) and the known triplet−triplet absorption spectrum of the $^3\pi\pi^*$ state of uridine 5′-monophosphate (UMP).[41] The latter spectrum has its maximum absorption near 400 nm and decreases slowly toward longer wavelengths. Our 1CHU transient spectrum recorded in acetonitrile 50 ps after the pump pulse (black trace, Figure 6) agrees well, particularly on the long-wavelength edge. This agreement indicates that the triplet state is already present 50 ps after excitation, but we postpone further discussion of ISC kinetics until later.

Significantly, the signals in protic solvents indicate the presence of another dark electronic state in addition to the $^3\pi\pi^*$ state. According to Figure 6, the $^3\pi\pi^*$ state of the uracil chromophore absorbs at both 340 and 550 nm. If only the triplet state were present, then signals at these wavelengths would show identical kinetics. If the triplet were formed rapidly enough, then VC dynamics could lead to differences at times $\lesssim$10 ps. In fact, the signals in Figure 4 at 340 and 500 nm are very clearly different for considerably longer times. The two signals agree only at times $\gtrsim$100 ps in water and $\gtrsim$1 ns in *n*-butanol. This shows that a second transient species or excited state is present in addition to the $^3\pi\pi^*$ state. The signals at these two wavelengths differ by the τ_4 decay, which is present at 340 nm but absent at 550 nm. This time constant varies strongly with solvent but is always much slower than the characteristic vibrational cooling time in each protic solvent. Thus, differences between 340 and 550 nm are not due to thermalization of excess vibrational energy but are instead assigned to a new electronic state that absorbs at 340 nm but absorbs negligibly at wavelengths greater than ~550 nm. In the following, we shall refer to this dark state, which is considerably shorter-lived than the $^3\pi\pi^*$ state, as the singlet dark state.

In aprotic solvents, the dark singlet state is more difficult to follow kinetically because it has a lifetime of at least several nanoseconds and is difficult to observe against the background of long-lived triplet states. Evidence for this lifetime is seen in the excess absorption between 350 and 450 nm in the transient spectrum of 1CHU versus UMP (Figure 6). The former spectrum recorded at 50 ps has contributions from both states, while only the triplet state contributes to the UMP spectrum, which was recorded on the microsecond time scale. In aerated ethyl acetate solution, the long-time signals decay much more slowly below 500 nm than they do at longer wavelengths. Since only the triplet absorbs at longer wavelengths, while both the singlet dark state and the triplet absorb at shorter wavelengths, this indicates once again that the dark singlet state persists for nanoseconds in aprotic solvents.

Dark State Yields. If S_0 absorbs more strongly at 252 nm than any other state present, then the bleach recovery signals measure the fraction of excited 1CHU molecules that have returned to the ground state as a function of time. This useful property of bleach signals was recently used to estimate the quantum yield of long-lived excited states in base-stacked oligonucleotides.[13] The fact that 1CHU signals are negative at 252 nm indicates that ground-state absorption is dominant, but there are good reasons to believe that absorption by other species is negligible. The molar absorption coefficient for 1CHU at 252 nm is ~5600 M^{-1} cm^{-1}. In contrast, the maximum molar absorption coefficient for the triplet of uridine 5′-monophosphate is ~1400 M^{-1} cm^{-1} at 400 nm.[42] Excited-state absorption by nucleobase $^1\pi\pi^*$ states, which absorb appreciably only at visible wavelengths, is far weaker still.[22] The $^1n\pi^*$ state, another

conceivable intermediate state (vide infra), is reported to have negligible absorption between 245 and 280 nm for a variety of monomethylated uracil compounds.[43]

Assuming that only S_0 absorbs at 252 nm, the fractional amplitude of the τ_2 decay is an estimate of the fraction of initial excited states that decay promptly via ultrafast internal conversion (IC) from the $^1\pi\pi^*$ state to S_0. This quantity is labeled the internal conversion yield to S_0, $\phi_{IC,0}$, in Table 4 and is ~60% in all protic solvents. The values in Table 4 differ slightly from the amplitudes presented in Tables 2 and 3 because the former values were calculated by averaging amplitudes for τ_2 from several independently measured transients. In ethyl acetate a somewhat lower yield is observed, while the yield is slightly higher in acetonitrile than that in the protic solvents. The fraction of the excited $^1\pi\pi^*$ population that does not undergo $^1\pi\pi^* \rightarrow S_0$ decay is given by $1 - \phi_{IC,0}$ and is therefore ~40% in all solvents. As we discuss next, this represents the fraction of initial excited states that decay via the two dark states: the triplet state and the state responsible for the τ_4 decay seen at 340 nm. The bleach recovery signal measured previously for TMP shows that approximately 10% of excitations decay to dark states.[13] It will be important for future studies to determine how this branching changes with the nature of the pyrimidine base.

The triplet yield was determined in similar fashion by averaging the fractional amplitude of the longest decay component from several independently measured transients at 252 nm (Table 4). Previous investigators have estimated triplet yields for a few uracil derivatives in various solvents using microsecond[44] and nanosecond flash photolysis,[10,11,45,46] sensitization,[44] and europium ion energy transfer.[47] These values are included in Table 4 for comparison. Although there is substantial scatter in the literature values, they show that ϕ_T increases significantly in solvents less polar than water, in agreement with the trend in Table 4 for 1CHU. The triplet yield in acetonitrile is 0.34 ± 0.06, a value 70% larger than the literature value of 0.2 for uracil in the same solvent.[10,11] The triplet yields in Table 4 for acetonitrile and ethyl acetate are likely to be overestimates because the dark singlet state lives for many nanoseconds in these less polar solvents, as described above. In protic solvents, the lifetime of the dark singlet state (τ_4 in Table 3) is short enough that its population has decayed completely to zero after 1 or 2 ns after the pump pulse and thus does not distort the triplet yield determined from the τ_3 amplitude. However, long-lived population in the singlet dark state still contributes to the residual bleach signal at long times in the aprotic solvents, causing ϕ_T to be overestimated.

Assignment of the Singlet Dark State. It is highly unlikely that the shorter-lived of the two dark states is a photoproduct or photoproduct precursor. In aqueous solution, uracil can react with a solvent molecule to yield a photohydrate.[48] In alcohols, an analogous addition reaction has been observed for 5-halopyrimidines but not for uracil itself. [49] The fraction of excited molecules that decay via the dark state is roughly 40% (Table 4), and it is difficult to envision a photoproduct or photoproduct precursor that could have the same yield in such a diverse set of solvents. The photohydrate yield for uracil in water is just 0.002.[50] We note further that the absence of a solvent kinetic isotope effect (Figure 5) rules out reactive steps in which proton transfer is rate-limiting. A second possible photoproduct is the cyclobutane pyrimidine dimer formed when two uracil molecules undergo $2\pi + 2\pi$ cycloaddition.[51] However, this reaction proceeds in dilute solution via the triplet state,[52] and at our concentrations diffusion is much too slow to produce the τ_4 decays that are clearly detectable 10 ps or so after excitation.

Assignment of the species responsible for the τ_4 decay to a triplet state was also considered. Calculations indicate that the second triplet state ($^3n\pi^*$) of uracil lies very close in energy to the $^1\pi\pi^*$ state.[5,53] The significant spin−orbit coupling calculated between these two states could facilitate ultrafast ISC,[5] suggesting that the τ_4 decay might be relaxation from the $^3n\pi^*$ to the lowest-energy $^3\pi\pi^*$ state. However, if τ_4 were due to internal conversion in the triplet manifold, then all of the population that enters the $^3n\pi^*$ state (~40%, as described earlier) should be trapped in the $^3\pi\pi^*$ state. This is inconsistent with the smaller and highly solvent-dependent triplet yields actually observed (Table 4).

We assign the τ_4 decay instead to a singlet excited state, which we argue is the lowest-energy $^1n\pi^*$ state. Very little spectroscopic evidence for $^1n\pi^*$ states of pyrimidines has been reported in the past. The absorption spectrum of crystalline 1-methyluracil was interpreted in terms of closely spaced $^1n\pi^*$ and $^1\pi\pi^*$ transitions.[54] Depolarization of the fluorescence anisotropy on the red edge of the lowest absorption band was assigned by Morgan and Daniels to the $^1n\pi^*$ state of thymine in room-temperature aqueous solution[55] but was later shown to be due to the more fluorescent thymine anion.[56]

The substantial yield (~40% in all solvents) of this nonradiative decay pathway is without precedent for nucleobases in the condensed phase. This demonstrates that a substantial fraction of photoexcited molecules do not relax to S_0 on a subpicosecond time scale. Of course, it has been known for many years that long-lived triplet (dark) states are formed by UV photoexcitation, but the yields are no greater than a few percent for any of the bases in aqueous solution.[9]

A recent computational study of nonradiative decay pathways in photoexcited uracil by Matsika[7] provides the key to interpreting our experimental results. In that work, the lowest singlet excited state (S_1) is the $^1n\pi^*$ state associated with excitation from the lone pair orbital on O8 to a π^* orbital.[7] The $^1n\pi^*$ state associated with the other oxygen atom (O7) lies over 1 eV higher in energy and is nearly isoenergetic with the second $^1\pi\pi^*$ state. This state ordering agrees with previous density functional theory/multireference configuration interaction calculations.[5] Importantly, Matsika located two distinct nonradiative decay pathways that are reached via passage through a sloped conical intersection (CI) between the lowest $^1\pi\pi^*$ state and the lowest $^1n\pi^*$ state. The geometry of uracil is still nearly planar at this CI. Nuclear motion along one of the two independent directions spanning the branching plane[57] leads to the minimum of the $^1n\pi^*$ surface, while motion along the other direction brings the molecule to a second CI with S_0. The former direction involves mostly stretching of the C4═O8 carbonyl group, while the pathway leading back to S_0 involves nonplanar deformations equivalent to twisting about the C5═C6 double bond.[7] Importantly, ethylene-like torsion about this bond has now been identified as a significant nonradiative decay coordinate for a variety of pyrimidine bases.[7,58−60]

The calculations for uracil show no barriers between the Franck−Condon point on the $^1\pi\pi^*$ state and the $^1\pi\pi^*/^1n\pi^*$ and the $^1\pi\pi^*/S_0$ CIs.[7] This suggests that both S_0 and the $^1n\pi^*$ state reached by decay from the $^1\pi\pi^*/^1n\pi^*$ CI can be reached on a picosecond or even femtosecond time scale. Our results provide the first experimental evidence for ultrafast branching or bifurcation in the optically bright $^1\pi\pi^*$ state of an excited nucleobase. We thus assign the singlet dark state seen in both protic and aprotic solvents to the lowest-energy $^1n\pi^*$ state. The τ_4 decay is assigned to the decay of this state to S_0. This follows from the good agreement between the inverted 252 nm transients

and the ones at 340 nm after the conclusion of vibrational cooling (Figure 4). It is unknown what is responsible for decay of the $^1n\pi^*$ state. The absence of a solvent kinetic isotope effect (Figure 5) rules out the possibility of rate-limiting proton transfer. Nevertheless, there is clear evidence that hydrogen bonding plays an important role since methanol and acetonitrile, which have similar dielectric constants, differ significantly in the lifetime of the $^1n\pi^*$ state.

Although this is the first time that "slow" nonradiative decay has been observed in solution, there is considerable evidence for long-lived excited states in gas-phase experiments on DNA and RNA bases. As discussed elsewhere,[2] the low-energy absorption spectra of a number of isolated bases include sharp resonances, particularly at low energy, which are consistent with long-lived states. In femtosecond transient ionization experiments, Kim and co-workers observed a long-lived component for thymine but not for uracil.[61] Particularly relevant is a report by Kong and co-workers, which showed that a variety of photoexcited uracil derivatives decay via an intermediate dark state in the gas phase.[43,62] These authors observed a state with a lifetime of between 20 and 200 ns in two-color resonance-enhanced multiphoton ionization experiments conducted with nanosecond lasers. On the basis of these lifetimes, they argued that a $^1n\pi^*$ state is responsible, although they could not rule out a triplet state. Our measurements, showing the simultaneous presence of the lowest triplet state and a second electronic state, strongly indicate that the state seen by Kong and co-workers is a $^1n\pi^*$ state. They suggested a lower limit of 20% for this channel in uracil,[62] which compares reasonably well with the ~40% branching yield seen here for 1CHU in all solvents.

Kong and co-workers observed that attachment of a single water molecule to thymine led to a strong decrease in the lifetime of the dark state.[43] They speculated that the solvent gives rise to the ultrashort lifetimes seen in condensed-phase experiments and suggested that it would be impossible to distinguish direct $^1\pi\pi^*$ to S_0 internal conversion from a cascade through the dark state. Our results show that neither of these suggestions about the condensed-phase behavior of uracil is correct. Although the lifetime of the dark state becomes steadily shorter on going from *n*-butanol to water (τ_4 in Table 3), the lifetime of this state in water (26 ps) is 2 orders of magnitude longer than the $^1\pi\pi^*$ state. This shows that hydration does not eliminate nonradiative decay via the singlet dark state. In fact, the lack of solvent dependence on bifurcation yields suggests that both pathways—ultrafast internal conversion to S_0 and branching to the $^1n\pi^*$ state—should be observable in the isolated molecule. Finally, we note that our results clearly differentiate between ultrafast IC to S_0 and a cascade via the $^1n\pi^*$ state since both pathways are simultaneously observable.

Given the evidence for a long-lived $^1n\pi^*$ state in solution (this work) and the gas phase,[43,62] it will be important to reexamine why time-resolved photoelectron spectroscopy studies have not identified this significant channel in thymine[6,63] or uracil.[63] The several picosecond decays seen in these studies, which were assigned to the decay of the $^1n\pi^*$ state,[6,63] are perhaps due to the substantial geometry change[7] that occurs in the $^1n\pi^*$ state.

Future computational studies must include dynamics to quantitatively capture the bifurcation event. Surprisingly, the branching appears to be independent of solvent, even though the energies of the $^1\pi\pi^*$ and $^1n\pi^*$ states at the ground-state geometry are known to shift relative to each other as solvent polarity is altered.[64] We suspect that whatever the state ordering at the Franck−Condon point, it is downhill on the $^1\pi\pi^*$ surface to a geometry where both states attain a conical intersection. An analogy could be drawn with the fluorescence lifetimes of the nucleobases, which are also strikingly independent of solvent properties.[2] This suggests that the dynamics are determined primarily by curvature of the $^1\pi\pi^*$ surface and not by solvation.

ISC Mechanism. The triplet yield in protic solvents (Table 4) increases as the lifetime of the singlet dark state increases (τ_4 in Table 3), suggesting at first glance that the $^3\pi\pi^*$ state of 1CHU is formed with rate τ_4^{-1} by decay of the dark singlet state, which we have argued above is the lowest-energy $^1n\pi^*$ state. However, no growth can be seen in transients at any wavelength with this time constant. Above 550 nm only the $^1\pi\pi^*$ state and the $^3\pi\pi^*$ state absorb. There is no absorption by the $^1n\pi^*$ state as the τ_4 decay component is completely absent. This is why this state went undetected in previous transient absorption experiments at visible probe wavelengths on uracil[20] and the other DNA and RNA bases.[21,22] Because the $^1\pi\pi^*$ state makes no contribution to these visible transients 1 ps after excitation, the long-time signals reflect only triplet population. The absence of rising signals at 550 nm, especially in solvents with substantial triplet yields, shows that the $^3\pi\pi^*$ state is populated at a rate greater than τ_4^{-1}.

There is an additional picosecond decay component (τ_2 in Tables 2 and 3), which contributes at visible wavelengths and appears between the decay of the $^1\pi\pi^*$ state (τ_1) and the long-time decay due to the $^3\pi\pi^*$ state (τ_3). The amplitude and time scale of this decay component are consistent with VC dynamics, but two observations rule out VC within S_0. First, the probe wavelengths are too far removed from the S_0 absorption band. Second, the lifetimes are distinctly different from the τ_2 values observed at UV probe wavelengths, shorter in acetonitrile and ethyl acetate but longer in the protic solvents. These observations indicate VC of either the dark singlet state or the $^3\pi\pi^*$ state—the only two species that absorb at visible wavelengths.

VC dynamics are clearly possible for the singlet dark state since it is formed on a subpicosecond time scale from the $^1\pi\pi^*$ state. However, it is conceivable that VC is taking place in the triplet state, and this would provide further support for ISC occurring in less than a few picoseconds. The τ_2 component in the aprotic solvents exhibits a rise near 400 nm and decays in the red wavelengths, suggestive of vibrational cooling in the $^3\pi\pi^*$ state, which has maximum absorption near 400 nm for UMP.[41] If this is correct, then the triplet must be formed more rapidly than the vibrational cooling time scale, which is ~10 ps in these solvents. The greater excess vibrational energy predicted for the $^3\pi\pi^*$ state compared to that of the $^1n\pi^*$ state in aqueous solution is another reason favoring assignment of τ_2 at visible probe wavelengths to thermalization of a rapidly formed triplet state. In aprotic solvents, the value of τ_2 (~4 ps) is significantly faster than at UV probe wavelengths, where this decay component is assigned to VC in the S_0 state. This could be due to the smaller amount of excess vibrational energy that must be transferred to the bath in the $^3\pi\pi^*$ state compared to S_0. It has been shown by varying the excitation wavelength that VC occurs more quickly as the amount of vibrational energy in a given electronic state is reduced.[65] Interestingly, τ_2 in the protic solvents with appreciable triplet yields (methanol and *n*-butanol) is also ~4 ps. The similar rates in both solvent groups for VC of the visible-absorbing state suggests that hydrogen bonding may be weaker in the $^3\pi\pi^*$ state and thus less effective at promoting intermolecular vibrational energy transfer to the solvent.

Having shown that triplet states are formed in no more than a few picoseconds, we next discuss how intersystem crossing

can occur so rapidly. Because intersystem crossing, like any other nonadiabatic step, depends strongly on nuclear coordinates, the amount of time that an excited molecule spends in a region of coordinate space with significant spin−orbit coupling could have a large effect on triplet yields. There are two possibilities for where ISC is most likely to take place: either before or after bifurcation. In the former case, initial motion along the nonradiative pathway in the $^1\pi\pi^*$ state could encounter regions of significant spin−orbit coupling, as suggested by recent calculations on cytosine.[66] There it was shown that favorable spin−orbit coupling is present along the minimum energy path that connects the minimum on the $^1\pi\pi^*$ surface with the conical intersection responsible for ultrafast internal conversion. In the case of ISC after bifurcation, the triplet state would be formed from an intermediate $^1n\pi^*$ state. We favor this scenario since the $^1n\pi^*$ state is expected to have high spin−orbit coupling according to El-Sayed's rules.[8] Furthermore, spin−orbit coupling along the initial $^1\pi\pi^*$ decay path is unlikely to change significantly with solvent, as we do not expect the topology of this path to change much with solvation.

To explain why the triplet is not formed during the entire lifetime of the $^1n\pi^*$ state (i.e., during the time τ_4 in protic solvents), we propose that the relaxed $^1n\pi^*$ state has negligible spin−orbit coupling with the $^3\pi\pi^*$ state compared to the initial $^1n\pi^*$ state with its excess vibrational energy. We postulate that spin−orbit coupling is significant only at early points along the nonradiative decay pathway. In the thermalized $^1n\pi^*$ state a barrier prevents this state from returning to regions with more favorable spin−orbit coupling. This terminates ISC even though the adiabatic energy of the $^1n\pi^*$ state is higher than that of the $^3\pi\pi^*$ state. Ultrafast internal conversion from the $^1\pi\pi^*$ state to the $^1n\pi^*$ state leaves the latter state with enough excess vibrational energy to overcome this barrier at early times, but the population quickly becomes trapped in the $^1n\pi^*$ state as VC takes place. Spin−orbit coupling in the relaxed $^1n\pi^*$ state may be smaller than that at early times due to the loss of planarity accompanying formation of the minimum energy $^1n\pi^*$ state.[7]

In this model, excess energy in the $^1n\pi^*$ state controls ISC dynamics. The triplet yield, which increases by nearly an order of magnitude on going from water to ethyl acetate, is not determined by the fraction of the population that enters the dark channel—this fraction is approximately constant in all solvents—but is determined instead by how quickly excess energy in the $^1n\pi^*$ state is dissipated to the solvent. Kinetically, it is difficult to tell whether ISC occurs directly from an earlier region along the nonradiative decay pathway prior to the $^1n\pi^*$ state or from the vibrationally hot $^1n\pi^*$ state since both are accessed so quickly. For this reason, quantum chemical calculations that calculate the spin−orbit coupling along the nonradiative decay pathways found for uracil[7] are urgently needed.

The ISC mechanism that we have proposed highlights a novel role for the solvent. In the past, there has been much discussion about how hydrogen-bonding solvents influence triplet yields in pyrimidines.[10,11,45,67] This discussion has focused on a hydrogen-bonding solvent's ability to tune the energy gap between $^1\pi\pi^*$ and $^1n\pi^*$ states. While energetics determine how much excess energy is initially present in the $^1n\pi^*$ state, we suggest that the solvent plays a crucial dynamical role by determining how long the molecule remains in regions of nuclear coordinate space with significant spin−orbit coupling. Thus, the accelerated rates of VC seen in hydrogen-bonding solvents (see earlier discussion) are responsible for the low triplet yields in protic solvents.

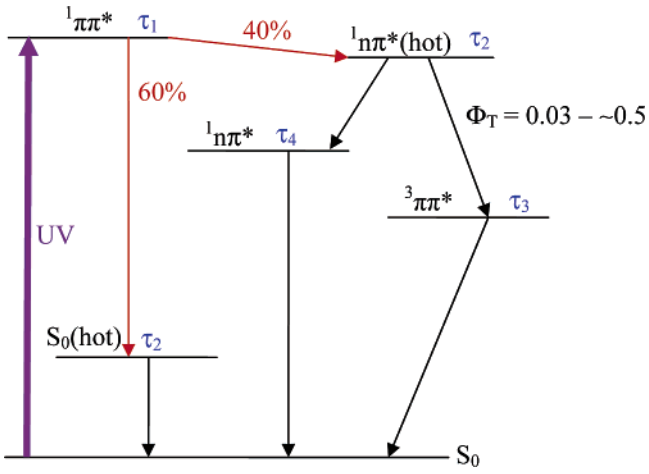

Figure 7. Jablonski diagram showing the proposed decay mechanism for photoexcited 1-cyclohexyluracil. The initial bifurcation is shown in red. The lifetime is shown next to each transient state in blue.

Adding ISC to the nonradiative pathways already discussed completes our schematic for photophysical decay in this uracil derivative (Figure 7). Although many details about triplet formation remain to be worked out, we believe that this model explains all current observations and a puzzling observation from the past—the wavelength dependence of ϕ_T for uracil. In aqueous solution, ϕ_T for uracil increases by a factor of 2 when the excitation wavelength is decreased from 260 to 230 nm.[47,50,68] Higher excitation energy could conceivably alter the fraction of the population that branches into the $^1n\pi^*$ state. It seems more likely, however, given the very different triplet yields observed already at a constant $^1n\pi^*$ population fraction of ~40% (Table 4) that shorter excitation wavelengths result in increased excess energy in the $^1n\pi^*$ state, leading to higher triplet yields. Since VC occurs more slowly when greater excess energy is present,[65,69] shorter excitation wavelengths increase the total time available to the hot $^1n\pi^*$ population to cross to the triplet state.

Conclusions

We have studied the excited-state dynamics of a uracil derivative in solvents with widely varying properties. The transient absorption signals reveal ultrafast branching in the initial bright state prepared by UV absorption. A fraction of the population decays via ultrafast internal conversion to S_0, but a significant fraction of ~40% decays to a dark $^1n\pi^*$ state, which decays to S_0 on a slower time scale. The earlier observation of a singlet dark state in TMP[13] suggests that this is a general feature of pyrimidine base photophysics. Importantly, a sizable number of triplets are formed in less polar solvents, which could have important consequences for DNA photochemistry. We have argued that ISC takes place only when sufficient excess energy is present in the $^1n\pi^*$ state. This study shows the power of the transient absorption technique for elucidating nonradiative decay pathways, including the dynamics of dark intermediate states. Fluorescence studies characterize the lifetime of the bright state,[16] but they do not provide information about the significant number of dark excited states that are reached nonradiatively. A complete picture of excited-state dynamics in uracil and in other pyrimidine bases must include the dark state decay.

Acknowledgment. This research was made possible by a grant from the National Institutes of Health (R01GM64563). Some measurements were performed in Ohio State's Center for

Chemical and Biophysical Dynamics, using equipment funded by the National Science Foundation and the Ohio Board of Regents. We thank Professor Robert W. Redmond for providing the triplet−triplet absorption spectrum of UMP shown in Figure 6.

References and Notes

(1) Callis, P. R. *Annu. Rev. Phys. Chem.* **1983**, *34*, 329.
(2) Crespo-Hernández, C. E.; Cohen, B.; Hare, P. M.; Kohler, B. *Chem. Rev.* **2004**, *104*, 1977.
(3) Broo, A. *J. Phys. Chem. A* **1998**, *102*, 526.
(4) Canuel, C.; Mons, M.; Piuzzi, F.; Tardivel, B.; Dimicoli, I.; Elhanine, M. *J. Chem. Phys.* **2005**, *122*, 074316.
(5) Marian, C. M.; Schneider, F.; Kleinschmidt, M.; Tatchen, J. *Eur. Phys. J. D* **2002**, *20*, 357.
(6) Samoylova, E.; Lippert, H.; Ullrich, S.; Hertel, I. V.; Radloff, W.; Schultz, T. *J. Am. Chem. Soc.* **2005**, *127*, 1782.
(7) Matsika, S. *J. Phys. Chem. A.* **2004**, *108*, 7584.
(8) El-Sayed, M. A. *Acc. Chem. Res.* **1968**, *1*, 8.
(9) Cadet, J.; Vigny, P. In *Bioorganic Photochemistry*; Morrison, H., Ed.; Wiley: New York, 1990; Vol. 1, p 1.
(10) Salet, C.; Bensasson, R. *Photochem. Photobiol.* **1975**, *22*, 231.
(11) Salet, C.; Bensasson, R.; Becker, R. S. *Photochem. Photobiol.* **1979**, *30*, 325.
(12) Cohen, B.; Hare, P. M.; Kohler, B. *J. Am. Chem. Soc.* **2003**, *125*, 13594.
(13) Crespo-Hernández, C. E.; Cohen, B.; Kohler, B. *Nature* **2005**, *436*, 1141.
(14) Reuther, A.; Laubereau, A.; Nikogosyan, D. N. *Opt. Commun.* **1997**, *141*, 180.
(15) Crespo-Hernández, C. E.; Kohler, B. *J. Phys. Chem. B* **2004**, *108*, 11182.
(16) Gustavsson, T.; Banyasz, A.; Lazzarotto, E.; Markovitsi, D.; Scalmani, G.; Frisch, M. J.; Barone, V.; Improta, R. *J. Am. Chem. Soc.* **2006**, *128*, 607.
(17) Taft, R. W.; Kamlet, M. J. *J. Am. Chem. Soc.* **1976**, *98*, 2886.
(18) Kamlet, M. J.; Abboud, J. L. M.; Abraham, M. H.; Taft, R. W. *J. Org. Chem.* **1983**, *48*, 2877.
(19) Connell, K. E.; Kurucsev, T.; Nordén, B. *Aust. J. Chem.* **1988**, *41*, 1509.
(20) Cohen, B.; Crespo-Hernández, C. E.; Kohler, B. *Faraday Discuss.* **2004**, *127*, 137.
(21) Pecourt, J.-M. L.; Peon, J.; Kohler, B. *J. Am. Chem. Soc.* **2000**, *122*, 9348.
(22) Pecourt, J.-M. L.; Peon, J.; Kohler, B. *J. Am. Chem. Soc.* **2001**, *123*, 10370.
(23) Peon, J.; Zewail, A. H. *Chem. Phys. Lett.* **2001**, *348*, 255.
(24) Gustavsson, T.; Sharonov, A.; Markovitsi, D. *Chem. Phys. Lett.* **2002**, *351*, 195.
(25) Gustavsson, T.; Sharonov, A.; Onidas, D.; Markovitsi, D. *Chem. Phys. Lett.* **2002**, *356*, 49.
(26) Terazima, M. *Chem. Phys. Lett.* **1999**, *305*, 189.
(27) Schwarzer, D.; Troe, J.; Votsmeier, M.; Zerezke, M. *J. Chem. Phys.* **1996**, *105*, 3121.
(28) Gochel-Dupuis, M.; Delwiche, J.; Hubin-Franskin, M.-J.; Collin, J. E. *Chem. Phys. Lett.* **1992**, *193*, 41.
(29) Koppel, I.; Molder, U.; Pikver, R. *Org. React.* **1983**, *20*, 45.
(30) Szczesniak, M.; Nowak, M. J.; Rostkowska, H.; Szczepaniak, K.; Person, W. B.; Shugar, D. *J. Am. Chem. Soc.* **1983**, *105*, 5969.
(31) Schoellhorn, H.; Thewalt, U.; Lippert, B. *J. Am. Chem. Soc.* **1989**, *111*, 7213.
(32) Maltese, M.; Passerini, S.; Nunziante-Cesaro, S.; Dobos, S.; Harsanyi, L. *J. Mol. Struct.* **1984**, *116*, 49.
(33) Tsuchiya, Y.; Tamura, T.; Fujii, M.; Ito, M. *J. Phys. Chem.* **1988**, *92*, 1760.
(34) Chin, S.; Scott, I.; Szczepani, K.; Person, W. B. *J. Am. Chem. Soc.* **1984**, *106*, 3415.
(35) Brown, R. D.; Godfrey, P. D.; McNaughton, D.; Pierlot, A. P. *J. Am. Chem. Soc.* **1988**, *110*, 2329.
(36) Millefiori, S.; Alparone, A. *Chem. Phys.* **2004**, *303*, 27.
(37) Yekeler, H.; Ozbakir, D. *J. Mol. Model.* **2001**, *7*, 103.
(38) Rejnek, J.; Hanus, M.; Labelac, M.; Ryjacek, F.; Hobza, P. *Phys. Chem. Chem. Phys.* **2005**, *7*, 2006.
(39) Morsy, M. A.; Al-Somali, A. M.; Suwaiyan, A. *J. Phys. Chem. B* **1999**, *103*, 11205.
(40) Daniels, M. *Proc. Natl. Acad. Sci. U.S.A.* **1972**, *69*, 2488.
(41) Gut, I. G.; Wood, P. D.; Redmond, R. W. *J. Am. Chem. Soc.* **1996**, *118*, 2366.
(42) Wood, P. D.; Redmond, R. W. *J. Am. Chem. Soc.* **1996**, *118*, 4256.
(43) He, Y.; Wu, C.; Kong, W. *J. Phys. Chem. A* **2004**, *108*, 943.
(44) Johns, H. E.; Whillans, D. W. *J. Am. Chem. Soc.* **1971**, *93*, 1358.
(45) Görner, H. *Photochem. Photobiol.* **1990**, *52*, 935.
(46) Nikogosyan, D. N.; Angelov, D. A.; Oraevsky, A. A. *Photochem. Photobiol.* **1982**, *35*, 627.
(47) Lamola, A. A.; Eisinger, J. *Biochim. Biophys. Acta* **1971**, *240*, 313.
(48) Fisher, G. J.; Johns, H. E. In *Photochemistry and Photobiology of Nucleic Acids*; Wang, S. Y., Ed.; Academic Press: New York, 1976; Vol. 1, p 169.
(49) Urjasz, W.; Maciejewski, A.; Celewicz, L. *Tetrahedron Lett.* **1999**, *40*, 3243.
(50) Brown, I. H.; Johns, H. E. *Photochem. Photobiol.* **1968**, *8*, 273.
(51) Fisher, G. J.; Johns, H. E. In *Photochemistry and Photobiology of Nucleic Acids*; Wang, S. Y., Ed.; Academic Press: New York, 1976; Vol. 1, p 225.
(52) Lamola, A. A.; Mittal, J. P. *Science* **1966**, *154*, 1560.
(53) Neiss, C.; Saalfrank, P.; Parac, M.; Grimme, S. *J. Phys. Chem. A* **2003**, *107*, 140.
(54) Eaton, W. A.; Lewis, T. P. *J. Chem. Phys.* **1970**, *53*, 2164.
(55) Morgan, J. P.; Daniels, M. *J. Phys. Chem.* **1982**, *86*, 4004.
(56) Williams, S. A.; Renn, C. N.; Callis, P. R. *J. Phys. Chem.* **1987**, *91*, 2730.
(57) Yarkony, D. R. *J. Phys. Chem. A* **2001**, *105*, 6277.
(58) Sobolewski, A. L.; Domcke, W. *Phys. Chem. Chem. Phys.* **2004**, *6*, 2763.
(59) Zgierski, M. Z.; Patchkovskii, S.; Lim, E. C. *J. Chem. Phys.* **2005**, *123*, 081101.
(60) Zgierski, M. Z.; Patchkovskii, S.; Fujiwara, T.; Lim, E. C. *J. Phys. Chem. A* **2005**, *109*, 9384.
(61) Kang, H.; Lee, K. T.; Jung, B.; Ko, Y. J.; Kim, S. K. *J. Am. Chem. Soc.* **2002**, *124*, 12958.
(62) He, Y.; Wu, C.; Kong, W. *J. Phys. Chem. A* **2003**, *107*, 5145.
(63) Ullrich, S.; Schultz, T.; Zgierski, M. Z.; Stolow, A. *Phys. Chem. Chem. Phys.* **2004**, *6*, 2796.
(64) Improta, R.; Barone, V. *J. Am. Chem. Soc.* **2004**, *126*, 14320.
(65) Laermer, F.; Elsaesser, T.; Kaiser, W. *Chem. Phys. Lett.* **1989**, *156*, 381.
(66) Merchán, M.; Serrano-Andrés, L.; Robb, M. A.; Blancafort, L. *J. Am. Chem. Soc.* **2005**, *127*, 1820.
(67) Görner, H. *J. Photochem. Photobiol., B* **1990**, *5*, 359.
(68) Johns, H. E. *Photochem. Photobiol.* **1968**, *7*, 633.
(69) Elsaesser, T.; Kaiser, W. *Annu. Rev. Phys. Chem.* **1991**, *42*, 83.
(70) *Handbook of Chemistry and Physics*, 74th ed.; Lide, D. R., Ed.; CRC Press: Boca Raton, FL, 1993.
(71) Fisher, G. J.; Varghese, A. J.; Johns, H. E. *Photochem. Photobiol.* **1974**, *20*, 109.